Available online at www.sciencedirect.com

ScienceDirect

Procedia IUTAM 15 (2015) 201 – 206

Procedia IUTAM

www.elsevier.com/locate/procedia

IUTAM Symposium on Multiphase flows with phase change: challenges and opportunities, Hyderabad, India (December 08 – December 11, 2014)

Evaporating falling drop

Manoj Kumar Tripathi[a,*], Kirti Chandra Sahu[a]

[a]*Department of Chemical Engineering, Indian Institute of Technology Hyderabad, Yeddumailaram 502 205, Andhra Pradesh, India*

Abstract

There-dimensional numerical simulations are carried out to investigate the dynamics of a drop undergoing evaporation and falling due to gravity. In order to accurately capture the interfacial phenomena dynamic adaptive grid refinement has been incorporated. The results are presented in terms of spatio-temporal evolution of the shape of the drop, along with the contours of the vapour concentration generated due to evaporation. This study has implications in natural phenomena, such as rainfall, dew formation and several industrial applications undergoing phase change. A parametric study of this phenomenon will be presented at the conference.

Peer-review under responsibility of Indian Institute of Technology, Hyderabad.

Keywords: Phase Change; Multiphase Flow, Bubbles & Drops, CFD

1. Introduction

Multiphase flows with phase-change are ubiquitous and have several industrial applications, for instance, energy generation, manufacturing, combustion. The dynamics of bubbles and drops is dominated by surface tension, where disjoint regions of one phase exist in another phase. Phase change in multiphase flows can occur due to chemical reaction, evaporation, melting, etc. In literature, several papers can be found discussing chemically reactive flows [1,2], which is not the subject of present discussion. In this case, when the temperature and pressure are favourable for the reaction to occur, a change in phase can take place and the mass of a new species (product of chemical reaction) increases at the expense of existing ones (reactants). In the present paper, we discuss the dynamics of a blob of heavier fluid falling under the action of gravity inside a lighter fluid initially kept at a higher temperature, and undergoing evaporation.

If the static pressure at the interface of the blob fluid is less (more) than the saturation vapour pressure at the given temperature, evaporation (condensation) can occur at the interface. Due to the relevance in many industrial applications, such as spray combustion, film evaporation and boiling, and naturally occurring phenomena in oceans and clouds, several investigations on evaporation/condensation have been conducted [3,4,5]. Phase change phenomena

* Manoj Kumar Tripathi. Tel.: +91-40-23016053
E-mail address: manoj@iith.ac.in

Peer-review under responsibility of Indian Institute of Technology, Hyderabad.
doi:10.1016/j.piutam.2015.04.028

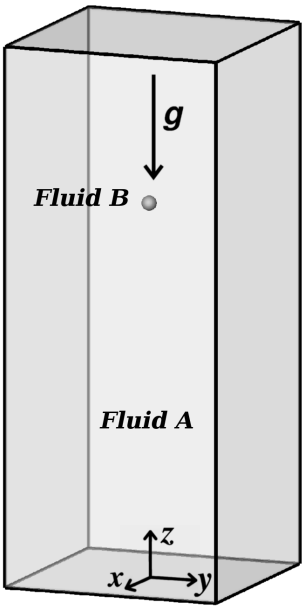

Fig. 1. The schematic showing the initial configuration of the drop of radius R. The inner and outer fluids are designated by B and A, respectively.

depend on several factors, including environmental conditions. Thus, computationally, it is an extremely difficult problem, and most of the previous studies are experimental in nature.

Recently, with increase in computational power many researchers have tried to incorporate phase-change models to their multiphase flow solvers[6,7,8,9,10]. Although accurate in describing the interface, the method of Esmaeeli & Tryggvason[7] is computationally expensive because of the explicit interface tracking and usage of linked lists for describing the elements on the interface. Workers in this area also have tried using one-fluid approaches, like volume-of-fluid (VOF), diffuse-interface and level-set methods to compute phase-change phenomena (see e.g Schlottke & Weigand[8]).

However, to the best of our knowledge the effect of viscosity and density ratios with temperature dependent fluid properties have not been investigated on falling drop undergoing evaporation. Recently, the dynamics of bubbles ($\rho_r b < 1$) and drops ($\rho_r b > 1$) has been studied by Tripathi et al.[11] under isothermal condition. Here $\rho_r b$ is the density ratio, defined in the next section. They showed that the dynamics of a bubble and drop is inherently different; although a drop can be made to behave as a mirror image of a bubble in the stokes flow regime when the viscosity ratio is adjusted based on certain criteria discussed in their paper.

In the present work, the effect of phase change on the dynamics of a falling drop is investigated for different viscosity and density ratios in three-dimensions. However, some results of a typical case corresponding to air-water system have been reported in this paper. An open-source code, Gerris, created by Popinet[12] is used and a phase-change model, similar to that of Schlottke & Weigand[8] is incorporated into Gerris in order to handle the complex phenomena occurring at the interface.

2. Formulation

We consider three-dimensional numerical simulation of a drop (at temperature T_c) of radius R falling under the action of gravity, g inside another fluid initially kept at a higher temperature (temperature T_h). The schematic showing the initial configuration of the drop is presented in Fig. 1. The inner and outer fluids are designated by 'B' and 'A', respectively. At time, $t = 0$ the drop is placed at a height, $H = 42R$ from the bottom of the computational domain of size $30R \times 30R \times 60R$. The viscosity and density ratios are defined as $\rho_{rb} \equiv \rho_B/\rho_A$ and $\mu_{rb} \equiv \mu_B/\mu_A$, respectively,

wherein ρ and μ represent density and viscosity, respectively. The Cartesian coordinate system (x, y, z) is used in order to formulate the problem, where x, y and z represent the horizontal, spanwise and vertical directions, respectively. The gravity is assumed to be acting in the negative z direction. The evaporation model is discussed below.

2.1. Evaporation model in the dimensional form

The interfacial mass source per unit volume, $\dot{m}_v$ is given by

$$\dot{m}_v = \mathcal{A}\left(\frac{\mathcal{D}_{av}\rho_g}{1-\omega}\right)\nabla\omega\cdot\hat{n}, \tag{1}$$

where $\mathcal{A}$ is the area of the interface per unit volume, and ω is the mass fraction of vapour inside the gas phase, given by

$$\omega = \frac{c_v\rho_v}{c_a\rho_g}, \tag{2}$$

where c_a and c_v are the volume fraction of dry air (fluid A) and vapour phase (which is set to zero everywhere at $t = 0$), respectively. The gas-liquid interface is assumed to be at the saturation condition, such that the gradient of vapour mass fraction across the interface can be estimated as,

$$\hat{n}\cdot\nabla\omega \approx \frac{\omega_n - \omega_{sat}}{x_n - x_{sat}}, \tag{3}$$

where x_n and x_{sat} are the locations of a neighbouring point lying in the gas phase and the location of the interface, respectively. Correspondingly, ω_n and ω_{sat} are the vapour mass fractions at x_n and x_{sat}, respectively.

The saturation vapour mass fraction is calculated, using Dalton's law of partial pressure, as

$$\omega_{sat} = M_{gv}\frac{p_{sat}}{p}, \tag{4}$$

where M_{gv} is the molar mass ratio of vapour to gas-mixture, p is the pressure field, and p_{sat} is the saturation vapour pressure depending on the local temperature as follows (employing the Wagner equation)

$$\ln\left(\frac{p_{sat}}{p_{cr}}\right) = \frac{a_1\tau + a_2\tau^{1.5} + a_3\tau^3 + a_4\tau^6}{1-\tau}, \tag{5}$$

where p_{cr} is the critical pressure, and $\tau = 1 - T/T_{cr}$, wherein T_{cr} is the critical temperature. For water, the coefficients $a_i (i = 1 \text{ to } 4)$ in the above equation are, $a_1 = -7.76451$, $a_2 = 1.45838$, $a_3 = -2.77580$ and $a_4 = -1.23303$. The critical pressure (p_{cr}) and temperature (T_{cr}) for water are 220.584 kPa and 647 K, respectively. The values of T_h and T_c are fixed at 343 K and 293 K, respectively.

2.2. Dimensionless governing equations

The dimensionless governing equations are given by

$$\nabla\cdot(\rho\mathbf{u}) = -\dot{m}_v, \tag{6}$$

$$\rho\left[\frac{\partial\mathbf{u}}{\partial t} + \mathbf{u}\cdot\nabla\mathbf{u}\right] = -\nabla p + \frac{1}{Ga}\nabla\cdot\left[\mu(\nabla\mathbf{u} + \nabla\mathbf{u}^T)\right] - \rho\vec{e}_z + \frac{\delta}{Bo}\left[\hat{n}\nabla\cdot\hat{n}\sigma + \nabla_s\sigma\right], \tag{7}$$

$$\frac{\partial c_a}{\partial t} + \nabla\cdot(\mathbf{u}c_a) = 0, \tag{8}$$

$$\frac{\partial(\rho c_p T)}{\partial t} + \nabla\cdot(\mathbf{u}\rho c_p T) = \frac{1}{GaPr}\nabla\cdot(\lambda\nabla T) - \frac{\dot{m}_v}{J_a}, \tag{9}$$

$$\frac{\partial c_v}{\partial t} + \nabla\cdot(c_v\mathbf{u}) = \nabla\cdot\left(\frac{1}{Pe}\nabla c_v\right) + \frac{\dot{m}_v}{\rho_{rv}}. \tag{10}$$

where $\mathbf{u}(u, v, w)$ and T represent the velocity and temperature fields, respectively, wherein u, v and w are the velocity components in the x, y and z, directions, respectively; t represents time; $\dot{m}_v$ is the mass source per unit volume; $Ga(\equiv \rho_A VR/\mu_A)$, $Pe(\equiv VR/\mathcal{D}_{av})$, $Ja(\equiv c_{p,A}(T_h - T_c)/\Delta h_v)$, $Pr(\equiv \rho_A c_{p,A}/\lambda_A)$ and $Bo(\equiv \rho_A g R^2/\sigma_0)$ denote the Galilei number, the Peclet number, the Jackob number, the Prandtl number and the Bond number, respectively. In Eq. (7), $\vec{e}_z$ is the unit vector in the vertical direction, $\delta(= |\nabla c_b|)$ is the Dirac distribution function, $\hat{n}(= -\nabla c_a/|\nabla c_a|)$ is the outward unit normal to the interface, and $\nabla_s(\equiv \nabla - \hat{\mathbf{n}}(\hat{\mathbf{n}} \cdot \nabla))$ is the surface gradient operator.

Eqs, (6)-(10) are dimensionless equations (written after dropping tildes), which are non-dimensionalized as

$$(x, y, z) = R\,(\widetilde{x}, \widetilde{y}, \widetilde{z})\,,\ t = \frac{R}{V}\widetilde{t},\ (u, v) = V(\widetilde{u}, \widetilde{v}),\ p = \rho_A V^2 \widetilde{p},$$

$$\mu = \widetilde{\mu}\mu_A,\ \rho = \widetilde{\rho}\rho_A,\ c_p = \widetilde{c}_p c_{p,A},\ \lambda = \widetilde{\lambda}\lambda_A,\ \sigma = \widetilde{\sigma}\sigma_0,\ \dot{m}_v = \dot{\widetilde{m}}_v \rho_A \sqrt{g/R},\ T = \widetilde{T}(T_h - T_c) + T_c,\ \delta = \frac{\widetilde{\delta}}{R}, \tag{11}$$

where the tildes designate dimensionless quantities, the velocity scale is $V = \sqrt{gR}$, and σ_0 is the surface tension at the liquid gas interface at reference temperature T_c.

The dimensionless density, viscosity, thermal conductivity and specific heat are given by

$$\rho = (1 - c_a)\rho_{rb} + [(c_a - c_v) + \rho_{rv} c_v]\,, \tag{12}$$

$$\mu = e^{-T}(1 - c_a)\mu_{rb} + \left(1 + T^{3/2}\right)[(c_a - c_v) + \mu_{rv} c_v]\,, \tag{13}$$

$$\lambda = (1 - c_a)\lambda_{rb} + [(c_a - c_v) + \lambda_{rv} c_v]\,, \tag{14}$$

$$c_p = \frac{(1 - c_a)c_{p,rb}\rho_{rb} + c_a\left[\frac{(c_a - c_v) + c_{p,rv} c_v \rho_{rv}}{(c_a - c_v) + \rho_{rv} c_v}\right]}{\rho}, \tag{15}$$

where $\rho_{rb} = \rho_B/\rho_A$, $\rho_{rv} = \rho_v/\rho_A$, $\mu_{rb} = \mu_B/\mu_A$, $\mu_{rv} = \mu_v/\mu_A$, $\lambda_{rb} = \lambda_B/\lambda_A$, $\lambda_{rv} = \lambda_v/\lambda_A$, $c_{p,rb} = c_{p,B}/c_{p,A}$ and $c_{p,rv} = c_{p,v}/c_{p,A}$, respectively. The dimensionless interfacial source term for mass transfer ($\dot{m}_v$) is given by

$$\dot{m}_v = \mathcal{A}\left(\frac{\rho_{rg}}{Pe(1 - \omega)}\right)\nabla\omega \cdot \hat{n}, \tag{16}$$

where $\rho_{rg} = \frac{c_v}{c_a}\rho_{rv} + \left(1 - \frac{c_v}{c_a}\right)$. In Eq. (7), surface tension of the liquid gas interface is given by the following constitutive equation

$$\sigma = 1 - \mathcal{M}_T T, \tag{17}$$

where $M_T = \gamma_T T_1/\sigma_0$.

2.3. Numerical method

In this work, Gerris[12], an open-source fluid flow solver, has been used to simulate the evaporating water drop falling under gravity. The Gerris source code has been modified to account for evaporation. The volumetric mass source term calculated from equation (16) is subtracted from the liquid phase and added to the gas phase. This modified mass source scaled with the densities of the liquid and gas phases serves as the volume source term for the continuity equation (6). This method is similar to the approach of Hardt & Wondra[13]. The drop dynamics is simulated using the volume-of-fluid (VoF) approach with dynamic adaptive grid refinement based on the vorticity magnitude, vapour concentration and bubble interface. This solver also minimizes the spurious currents at the interface (which are known to appear when the density and the viscosity ratios are high) by incorporating a balanced force continuum surface force formulation[14] for the inclusion of the surface force term in the Navier-Stokes equations.

The dynamic adaptive mesh refinement feature of Gerris comes as a great advantage in this problem as it allows us to maintain the distributed source term within a thin region near the interface. This helps in obtaining a good approximation to a sharp mass source located at the interface[8] and one does not require to modify the VoF advection equation (equation (8)). The solver has been validated by comparing with several known numerical and experimental results for rising bubble and falling drop problems[15,16].

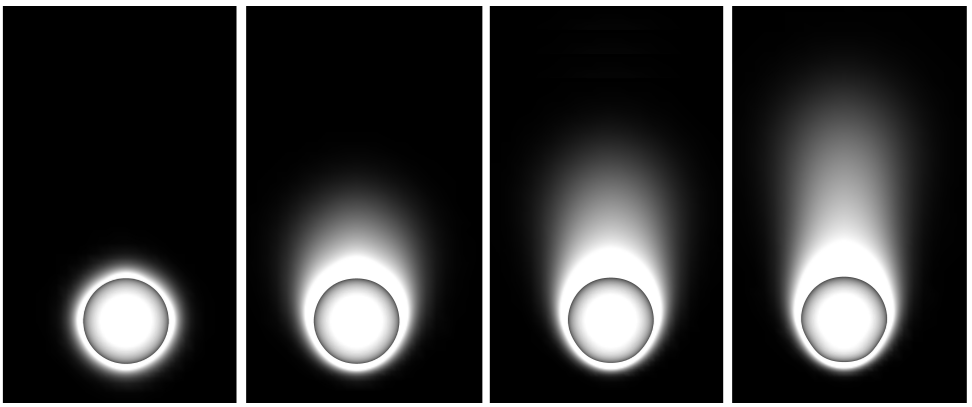

Fig. 2. The time evolution of shape of the drop along with the vapour volume fraction obtained using the parameter values $\rho_{rb} = 1000$, $\mu_{rb} = 55$, $\rho_{rv} = 0.9$, $\mu_{rv} = 0.7$, $\lambda_{rb} = 26$, $\lambda_{rv} = 1$, $c_{p,rb} = 4$, $c_{p,rv} = 2$, $Ga = 50$, $Bo = 0.1$, $Pr = 10$, $Pe = 10$, $Ja = 50$, and $\mathcal{M}_T = 0.2$. From left to right: t =0.5, 2, 2.5 and 3. The maximum value of the contour level is 3×10^{-4}.

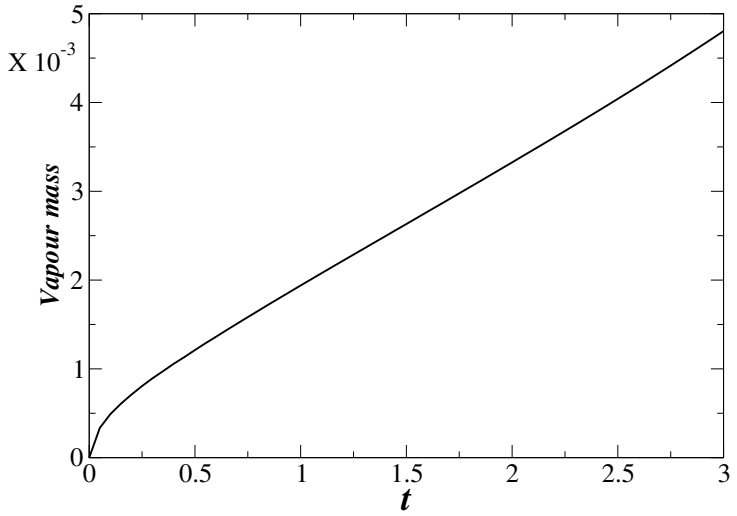

Fig. 3. Mass of the vapour versus time for the parameter values the same as those used in Fig. 2.

3. Results and Discussion

The time evolution of the shape of the drop and the contours of vapour volume fraction obtained for $\rho_{rb} = 1000$, $\mu_{rb} = 55$, $\rho_{rv} = 0.9$, $\mu_{rv} = 0.7$, $\lambda_{rb} = 26$, $\lambda_{rv} = 1$, $c_{p,rb} = 4$, $c_{p,rv} = 2$, $Ga = 50$, $Bo = 0.1$, $Pr = 10$, $Pe = 10$, $Ja = 50$, and $\mathcal{M}_T = 0.2$ are shown in figure 2. It can be seen that as the time progresses the shape of the drop tends to elongate in the lateral direction. Due to the evaporation, a circular shaped envelope of liquid vapour is formed at the initial time (e.g. see the result at $t = 0.5$ in figure 2). The amount of vapour produced keeps on increasing as the time progresses (see figure 3). As the drop moves in the downward direction a wake region is created at the upper part of the drop, which increases the evaporation rate in the low pressure region. Also the vapour produced at the bottom part of the drop moves into the wake region due to buoyancy, thus creating a 'fore-aft' asymmetric vapour envelope (shown at later times). It can also be seen that the drop has been deformed slightly to an oblate shape as it moves in the downward direction.

4. Conclusion

The three-dimensional dynamics of a falling drop under the action of gravity and undergoing evaporation is investigated using an open-source code, Gerris. Our three-dimensional simulation reveals that as time progress a a 'fore-aft' asymmetric vapour envelope is produced due to the propagation of the vapour towards the wake region behind the drop, and due to preferential evaporation in low pressure region. We expect to observe vortex shedding in the contour of vapour at later times. Parametric study of our three-dimensional simulations will be presented at the meeting.

Acknowledgement

The authors gratefully acknowledged Professor Rama Govindarajan for valuable suggestions. They also thank Indian Institute of Technology Hyderabad for providing support.

References

1. T. R. Bussing and E. M. Murman, "Finite-volume method for the calculation of compressible chemically reacting flows," AIAA J. **26**, 1070 (1988).
2. V. Moureau *et al.*, "Numerical methods for unsteady compressible multi-component reacting flows on fixed and moving grids," J. Comput. Phys **202**, 710 (2005).
3. H. L. Penman, "Natural evaporation from open water, bare soil and grass," Proceedings of the Royal Society of London. Series A. Mathematical and Physical Sciences **193**, 120 (1948).
4. D. Brutin, B. Sobac, B. Loquet, and J. Sampol, "Pattern formation in drying drops of blood," J. Fluid Mech. **667**, 85 (2011).
5. G. Lagubeau, M. Le Merrer, C. Clanet, and D. Quéré, "Leidenfrost on a ratchet," Nature Physics **7**, 395 (2011).
6. D. Juric and G. Tryggvason, "Computations of boiling flows," Int. J. Multiphase Flow **24**, 387 (1998).
7. A. Esmaeeli and G. Tryggvason, "Computations of film boiling. Part I: numerical method," Int. J. Heat Mass Transfer **47**, 5451 (2004).
8. J. Schlottke and B. Weigand, "Direct numerical simulation of evaporating droplets," J. Comput. Phys **227**, 5215 (2008).
9. I. Chakraborty, G. Biswas, and P. Ghoshdastidar, "A coupled level-set and volume-of-fluid method for the buoyant rise of gas bubbles in liquids," Int. J. Heat Mass Transfer **58**, 240 (2013).
10. P. J. Saenz *et al.*, "On phase change in Marangoni-driven flows and its effects on the hydrothermal-wave instabilities," Phys. Fluids **26**, 024114 (2014).
11. M. K. Tripathi, K. C. Sahu, and R. Govindarajan, "Why a falling drop does not in general behave like a rising bubble," Scientific reports **4**, (2014).
12. S. Popinet, "Gerris: a tree-based adaptive solver for the incompressible Euler equations in complex geometries," J. Comput. Phys **190**, 572 (2003).
13. S. Hardt and F. Wondra, "Evaporation model for interfacial flows based on a continuum-field representation of the source terms," J. Comput. Phys **227**, 5871 (2008).
14. J. Brackbill, D. B. Kothe, and C. Zemach, "A continuum method for modeling surface tension," J. Comput. Phys **100**, 335 (1992).
15. M. Sussman and P. Smereka, "Axisymmetric free boundary problems," J. Fluid Mech. .
16. D. Bhaga and M. E. Weber, "Bubbles in viscous liquids: shapes, wakes and velocities," J. Fluid Mech. **105**, 61 (1981).